THE EFFECT OF GROUND ICE REDISTRIBUTION ON THE MARTIAN PALEO-CO2 CYCLE. E. David[1], O. Aharonson[1,2], E. Vos[1], F. Forget[3] and N. Schorghofer[2], [1]Weizmann Institute of Science, Rehovot, Israel (elad.david@weizmann.ac.il), [2]Planetary Science Institute, Tucson, Arizona / Honolulu, Hawaii [3]Laboratoire de Météorologie Dynamique, Jussieu, Paris, France.

Introduction: CO_2 is the major constituent of the atmosphere of Mars, comprising ~95% of its composition [1]. Seasonal CO_2 surface-atmosphere exchange results in pressure variations of 25-30% [2]. Shallow perennial ground water ice, which exists throughout mid- and high latitudes [3,4,5], acts as a heat sink during the spring/summer months and as a heat source during autumn/winter due to its high thermal conductivity. The increase in wintertime surface temperatures results in inhibition of CO_2 accumulation and an increase in atmospheric pressure [6].

The distributions of both the seasonal CO_2 and ground ice evolve with the secular changes of the orbital parameters, namely eccentricity (e), longitude of perihelion (L_p) and obliquity (ε), on timescales on 10's-100's kyr [7]. Ground ice extends to lower latitudes with increasing obliquity as humidity grows, and recedes poleward with decreasing obliquity [8,9]. Similarly, the seasonal CO_2 caps extend equatorward with increasing obliquity, accompanied by intensifying seasonal pressure variations, and withdraw to high latitudes as obliquity declines [10,11]. In this work, we provide a qualitative analysis of the effect of orbitally-forced ground ice redistributions on the long-term evolution of the seasonal CO_2 cycle throughout the recent history of Mars.

Methods & Results: We use the Global Climate Model developed by the Laboratoire de M'et'eorologie Dynamique, CNRS, Paris (LMD-GCM) [12] to simulate the paleoclimate with different orbital parameters and ground ice distributions, at a 64x64x29 grid (resolution of 2.8125º latitude and 5.625º longitude). To calculate the equilibrium ground ice distribution at each orbital configuration, we use the Mars Subsurface Ice Model (MSIM), a one-dimensional thermal equilibrium model [13], https://github.com/nschorgh/MSIM/. The model calculates the depth of an ice table in diffusive equilibrium with the atmosphere under a dry regolith layer. We compare the CO_2 cycle from pairs of GCM simulations, which are identical in all aspects except for the ground ice distribution: in one simulation we use a fixed reference distribution (based on MONS observations [4,5]) independent of orbital configuration ("MONS GI"); in the second, we use the MSIM ground ice predicted distribution, which is in equilibrium with the instantaneous orbital configuration ("Eq. GI"). Ground ice is represented in the GCM as elevated thermal inertia (I), with the relation between pore filling fraction and thermal inertia following a previous formulation [13]. The pore space (with porosity $\Phi = 0.4$) is ice-cemented under the ice table, as expected in a state of full diffusive equilibrium. We present results of simulations for obliquity $\geq 30º$, which have reached steady state. At obliquity $\leq 25º$ our simulations do not converge due to the continued accumulation of CO_2 ice at the poles (however, we note that we expect the choice of ground ice scenario to have little effect on the CO_2 cycle at these obliquities because in both ground ice distributions, the seasonal cap is almost entirely underlain by ground ice).

Figure 1 shows maps of total seasonal CO_2 column density (kg/m^2) at obliquity 45º in the Eq. GI and MONS GI scenarios, and difference in accumulation between scenarios. As obliquity increases, the seasonal cap extends to lower latitudes, overtaking the present-day margin of the ground ice. In the MONS GI scenario, the seasonal cap at mid-latitudes is

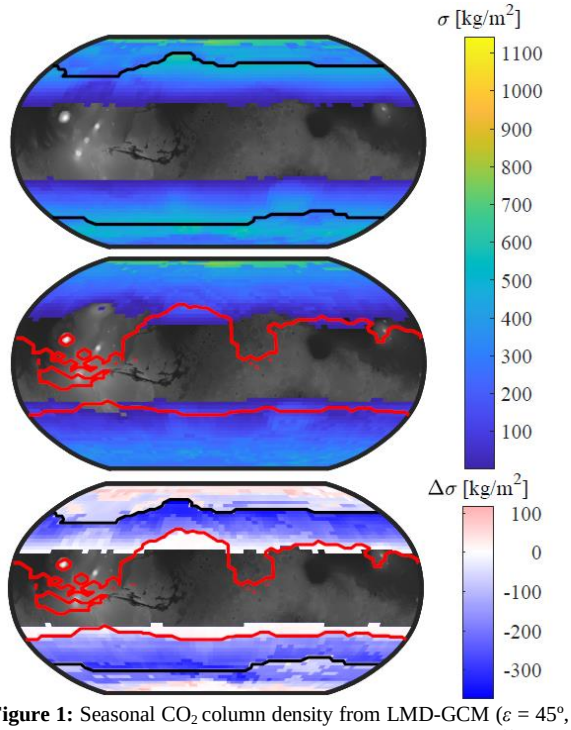

Figure 1: Seasonal CO_2 column density from LMD-GCM (ε = 45º, e = 0) with MONS GI (top), Eq. GI (middle) and difference between scenarios (Eq. GI – MONS GI, bottom). Ground ice margins are marked by contour.

uninhibited by ground ice; accumulation increases abruptly at latitudes equatorward of the MONS ground ice margins. In contrast, equilibrium ground ice migrates equatorward at higher obliquities, acting to inhibit accumulation and decreasing the seasonal duration of surface CO_2 at mid-latitudes. This results in a monotonic decline of seasonal surface CO_2 mass from pole to equator in the Eq. GI scenario, in contrast to the MONS GI scenario. Notice that at high obliquity ground ice is stabilized in regions of low thermal inertia. The presence of shallow ground ice at the margins of the seasonal caps results in their retreat, mainly in the northern hemisphere (most notably in Tharsis, Arabia and Elysium). It is possible that these regions have not experienced seasonal CO_2 accumulation for at least the past 20 Ma.

Figure 2 shows the seasonal variations of the global mean surface pressure for both the Eq. GI and MONS GI scenarios between obliquity 30º to 45º. As expected, ground ice equatorward migration attenuates the increasing pressure variations with rising obliquity. With increasing obliquity, the two ground ice scenarios diverge. Ground ice redistribution results in a decrease of the seasonal pressure amplitude by ~20%/40% for obliquity 30º/45º, respectively, relative to the amplitude in the MONS GI scenario. Ground ice migration mainly affects the depth of the seasonal pressure minima, reducing the differences among them, and hence maintaining the mean annual pressure roughly constant throughout high obliquity periods.

We run the GCM for an array of 52 discrete orbital parameters within the range of the past 20 Ma, excluding obliquity ≤ 25º ($0 \le e \le 0.12$, $0º \le L_p \le 360º$, $30º \le \varepsilon \le 45º$) for the two ground ice scenarios. We then interpolate these results according to the computed orbital parameters for the past 20 Ma [7]. In Figure 3, we show a section of this evolution during a period of high obliquity between 6000 kya and 8000 kya. The incorporation of migrating ground ice limits the seasonal surface pressure variations (ΔP) to no more than 200 Pa, whereas in the non-migrating ground ice scenario surface pressure amplitude reaches values of over 300 Pa.

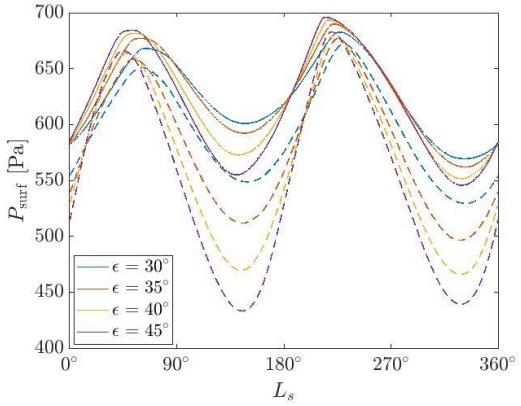

Figure 2: Global mean surface pressure as a function of areocentric longitude L_s at different obliquities. Eq. GI scenario is shown in solid lines, MONS GI scenario in dashed.

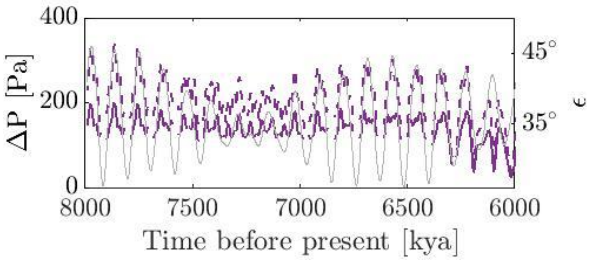

Figure 3: Interpolated seasonal surface pressure amplitude for a period of high mean obliquity between 6000 kya and 8000 kya, for the Eq. GI (solid) and MONS GI (dashed) scenarios. Obliquity is shown in gray. Only results for $\varepsilon \geq 30º$ are presented.

Discussion: Our work highlights the role of ground ice migration on the paleoclimate of Mars as an attenuator of large surface and atmospheric CO_2 variations, particularly at high obliquity as the seasonal cap extends further from modern day ground ice, and suggests potentially significant implications on the modelling of recent Mars. We are currently advancing this analysis to explore the effect of ground ice redistribution on the overall climate system. Changes in the seasonal caps' mass and duration may influence the planetary energy budget and general circulation, potentially affecting dust lifting and volatile transport. Finally, more complex scenarios may be considered, such as non-equilibrium ground ice, ground ice in the presence of an equatorial humidity source, and others.

Acknowledgments: The authors wish to thank the Helen Kimmel Center for Planetary Sciences, ISF Grant #137578 for support of this work and Paul Hayne for helpful discussions.

References: [1] Owen, T., et al. (1977) *JGR*. 4635-4639. [2] Tillman, J. E., et al. (1993) *JGR*, 98(E6), 10963-10971. [3] Squyres, Steven W., et al. (1986) *Science*, *231*(4735), 249-252. [4] Boynton, W. V., et al. (2002) *Science*, *297*(5578), 81-85. [5] Feldman, W. C., et al. (2002) *Science*, *297*(5578), 75-78. [6] Haberle, R. M., et al. (2008) *PSS*, *56*, 251-255. [7] Laskar, J., et al. (2004) *Icarus*, *170*, 343-364. [8] Mellon, M. T., & Jakosky, B. M. (1995) *JGR*, *100*, 11781-11799. [9] Chamberlain, M. A., & Boynton, W. V. (2007) *JGR*, *112*, E06009. [10] Toon, O. B., et al. (1980) *Icarus*, *44*, 552-607. [11] Mischna, M. A., et al. (2003) *JGR*, *108*(E6), 5062. [12] Forget, F., et al. (1999) *JGR*, *104*, 24155-24175. [13] Schorghofer, N., & Aharonson, O. (2005) *JGR*, *110*, E05003.